PHARMACEUTICAL BIOLOGY
2023, VOL. 61, NO. 1, 249–258
https://doi.org/10.1080/13880209.2023.2166966

Taylor & Francis
Taylor & Francis Group

RESEARCH ARTICLE

OPEN ACCESS Check for updates

Chaihu Shugan San promotes gastric motility in rats with functional dyspepsia by regulating Drp-1-mediated ICC mitophagy

Li Li*, Qingling Jia*, Xiangxiang Wang, Yujiao Wang, Chenheng Wu, Jun Cong and Jianghong Ling

Shuguang Hospital, Shanghai University of Traditional Chinese Medicine, Shanghai, People's Republic of China

ABSTRACT

Context: Chaihu Shugan San (CHSGS) was effective in the treatment of functional dyspepsia (FD).

Objective: To investigate the mechanism of CHSGS in FD through dynamin-related protein 1 (Drp-1)-mediated interstitial cells of cajal (ICC) mitophagy.

Materials and methods: Forty Sprague-Dawley (SD) rats were randomly divided into control, model, mdivi-1, mdivi-1 + CHSGS and CHSGS groups. Tail-clamping stimulation was used to establish the FD model. Mdivi-1 + CHSGS and CHSGS groups were given CHSGS aqueous solution (4.8 g/kg) by gavage twice a day. Mdivi-1 (25 mg/kg) was injected intraperitoneally once every other week for 4 w. Mitochondrial damage was observed by corresponding kits and related protein expressions were assessed by Immunofluorescence and (or) Western Blot.

Results: Compared with the mean value of the control group, superoxide dismutase (SOD) and citrate synthase (CS) in the model group were decreased by 11% and 35%; malondialdehyde (MDA) and reactive oxygen species (ROS) were increased by 1.2- and 2.8-times; ckit fluorescence and protein expressions were decreased by 85% and 51%, co-localization expression of LC3 and voltage dependent anion channel 1 (VDAC1), Drp-1 and translocase of the outer mitochondrial membrane 20 (Tom20) were increased by 10.1- and 5.4-times; protein expressions of Drp-1, Beclin-1, and LC3 were increased by 0.5-, 1.4-, and 2.5-times whereas p62 was decreased by 43%. After mdivi-1 and (or) CHSGS intervention, the above situation has been improved.

Discussion and conclusion: CHSGS could improve mitochondrial damage and promote gastric motility in FD rats by regulating Drp-1-mediated ICC mitophagy.

ARTICLE HISTORY
Received 26 August 2022
Revised 24 November 2022
Accepted 5 January 2023

KEYWORDS
Chinese medicine formula; functional gastrointestinal diseases (FGIDs); mdivi-1

Introduction

Functional dyspepsia (FD) is the common clinical digestive disorder, mainly manifested by pain or burning sensation in the upper abdomen, postprandial abdominal fullness and early satiety (Madisch et al. 2018). Epidemiological data show that the prevalence of FD is as high as 10% worldwide, and the incidence is increasing year by year, which seriously affects the quality of patients' life (Barberio et al. 2020; Ford et al. 2020). The pathogenesis of FD is not yet clear, and gastric motility disorder is one of the classical pathogeneses of FD, which plays an important role in the formation and development of FD (Wauters et al. 2020).

Mitophagy is a normal physiological activity of cells and one of the forms of autophagy (Mizushima and Komatsu 2011). Mitochondrial division inhibitor (Mdivi-1) is a mitochondrial division protein inhibitor that inhibits dynamin-related protein 1 (Drp-1) self-assembly and mitochondrial division by inhibiting GTPase activity (Liu et al. 2020; Ding et al. 2022). Drp-1 is a key protein that regulates mitochondrial division, and its overexpression leads to accelerated mitochondrial division and accelerated mitophagy, which in turn exacerbates gastrointestinal motility disorders (Rovira-Llopis et al. 2017).

Chaihu Shugan San (CHSGS) is a classical formula for destressing the liver and relieving depression, promoting qi and relieving pain, and strengthening the spleen and harmonizing the stomach. Our group is committed to the study of the therapeutic mechanism of CHSGS in the treatment of FD (Tan et al. 2019). The results of previous experiments showed that FD rats showed a large number of autophagic vesicles along with mitochondrial swelling and even vacuolization (Zhang et al. 2018), and CHSGS could inhibit excessive autophagy of ICC in gastric tissue of FD rats and exert a pro-gastric motility effect (Tan et al. 2019). Although it is known that CHSGS could reduce ICC autophagy in FD rats, its specific mechanism has rarely been investigated. Therefore, we explored the mechanism of CHSGS to improve mitochondrial damage and promote gastric motility in FD rats through Drp-1-mediated ICC mitophagy.

Materials and methods

Animals

Forty specific pathogen-free (SPF) Sprague-Dawley (SD) rats (210 ± 10 g), were purchased from Zhejiang Weitong Lihua Laboratory Animal Technology Co., Ltd., housed in SPF-grade barrier environment at the Experimental Animal Center of Shanghai University of Traditional Chinese Medicine (TCM),

CONTACT Jianghong Ling ljh18817424778@163.com Shuguang Hospital, Shanghai University of Traditional Chinese Medicine, Shanghai 200021, People's Republic of China
*These authors contributed equally to this work.

with alternating 12 h light and dark cycles, relative temperature 22 ± 2 °C, and relative humidity 55 ± 2%. This study was approved by the Animal Ethics Committee of Shanghai University of TCM (PZSHUTCM210625006).

CHSGS and its preparation

CHSGS was provided by Shuguang Hospital affiliated to Shanghai University of TCM. According to the proportion of the original formula, 16 g each of Bupleuri Radix (*Curcuma phaeocaulis* Val. [Gingeraceae], Chaihu) and Citri Reticulatae Pericarpium (*Cirtus reticulata* Blanco [Rutaceae], Chenpi), 12 g each of Paeoniae Radix Alba (*Paeonia lactiflora* Pall. [Ranunculaceae], Baishao), Chuanxiong Rhizoma (*Ligusticum chuanxiong* Hort. [Umbelliferae], Chuanxiong), Aurantii Fructus Immaturus (*Citrus aurantium* L. [Rutaceae], Zhishi), and Cyperi Rhizoma (*Cyperus rotundus* L. [Cyperaceae], Xiangfu), and 4 g of Glycyrrhizae Radix et Rhizoma Praeparata cum Melle (*Glycyrrhiza uralensis* Fisch. [Leguminous], Zhi Gan Cao) were weighed, soaked in distilled water for 30 min, boiled on high heat, and decocted on low heat for 30 min; the decoction was combined after 2 repetitions, and evaporated to 175 mL by heating in a water bath, stored in a refrigerator at 4 °C, and made into aqueous decoction concentrate with a raw drug concentration of 0.48 g/mL and re-decocted every 2 d.

Reagents

Mdivi-1 (S7162) was purchased from Shanghai Selleck (Shanghai, China). Rabbit anti-Drp-1 (ab184247) was from Abcam (Cambridge, UK). Rabbit anti-ckit (3074), rabbit anti-Beclin-1 (3738S), rabbit anti-p62 (23214S), rabbit anti-LC3 (4108S), mouse anti-β-actin (3700S), anti-rabbit IgG, HRP-linked antibody (7074P2), and anti-mouse IgG, HRP-linked antibody (7076P2) were purchased from Cell Signaling Technology (MA, USA). Mouse anti-voltage dependent anion channel 1 (VDAC1) (sc-390996), and mouse anti-outer mitochondrial membrane 20 (Tom20) (sc-17764) were provided by Santa Cruz Biotechnology, Inc., (CA, USA). Bovine serum albumin (BSA) (ST023), alexa fluor 488-labeled goat anti-rabbit IgG (H + L) (A0423), Cy3-labeled goat anti-rat IgG (H + L) (A0507), antifade mounting medium with 4′,6-diamidino-2-phenylindole (DAPI) (P0131), and sodium dodecyl sulfate-polyacrylamide gel electrophoresis (SDS-PAGE) gel quick preparation kit (P0012AC) were from Shanghai Beyotime Biotechnology Co., Ltd., (Shanghai, China). Mitochondrial extraction kit (SM0020) was purchased from Beijing Solarbio Science & Technology Co., Ltd., (Beijing, China). EZ-Buffers H 10X tris buffered saline with tween 20 (TBST) buffer (C520009) was from Shanghai Sangon Biotech Co., Ltd., (Shanghai, China). Rat citrate synthase (CS) enzyme linked immunosorbent assay (ELISA) kit (EK-R30678) was purchased from Shanghai Enzyme research Biological Technology Co., Ltd., (Shanghai, China). Reactive oxygen species (ROS) assay kit (E004-1-1), superoxide dismutase (SOD) assay kit (A001-3-2), and malondialdehyde (MDA) assay kit (A003-1-2) were provided by Nanjing Jiancheng Bioengineering Institute (Nanjing, China).

Grouping, modelling and drug administration

After 1 week of adaptive feeding, 40 SD rats were randomly divided into control group (C), model group (M), mdivi-1 group (mdivi-1), mdivi-1 + Chaihu Shugan San group (mdivi-1 + CHSGS), and Chaihu Shugan San group (CHSGS), 8 rats in each group. All groups, except the control group, were modelled with reference to the modified tail-clamping stimulation method (Wu et al. 2020; Hou et al. 2022) for 30 min each time, 2 times/d for 4 week. Based on the previous study, the effect was better in the CHSGS group at a dose of 4.8 g/kg (Zhang et al. 2018), so the mdivi-1 + CHSGS and CHSGS groups were given 4.8 g/kg aqueous solution, and the model group was given the same volume of normal saline at 1.0 mL/100 g by gavage once in the morning and once in the evening at an interval of 12 h for 4 w. Mdivi-1 was injected intraperitoneally once every other week at a dose of 25 mg/kg.

Preparation of semi-solid paste

Dissolved 5 g of sodium carboxymethyl cellulose, 8 g of skim milk powder, 4 g of starch and 4 g of sugar in 125 mL of distilled water, mixed thoroughly to make 150 mL of nutritional semi-solid paste (Zhang et al. 2018).

Specimen collection and processing

After the last administration, the rats were fasted for 12 h. On the following day, the rats were gavaged with semi-solid paste and anesthetized with 2% sodium pentobarbital after 30 min. The whole stomach was exposed, and the cardia and pylorus were quickly ligated with surgical wires, the connective tissues on the surface of the stomach were stripped, and the mass of the whole stomach was weighed, the stomach was cut along the greater curvature and contents were rinsed with saline, the mass of the empty stomach was weighed after wiping dry with filter paper. The gastric sinus tissue was partially placed in 5% glutaraldehyde and 4% paraformaldehyde for fixation and storage, and the mitochondria were partially extracted according to the instructions of the mitochondrial extraction kit, and the rest was stored in the refrigerator at −80 °C.

Determination of gastric emptying rate and small intestinal propulsion rate by semi-solid paste method

Calculations were performed according to the following formula: gastric emptying rate = [1 – (whole stomach mass – empty stomach mass)/semi-solid paste mass] × 100%, small intestine propulsion rate (%) = distance of semi-solid paste advanced in small intestine/total length of small intestine × 100% (Liang et al. 2018; Zhu et al. 2020).

Histopathological changes in rat gastric antrum tissue observed by HE staining

After the slices were dewaxed, hematoxylin staining was performed for 2 min, eosin staining for 90 s oven at 60 °C for 30 min, and neutral resin sealing to observe the histopathological changes of gastric antrum sinus (Yi et al. 2022).

Determination of mitochondrial SOD content in rat gastric tissues by WST-1 method

The mitochondria of fresh gastric tissue were taken, operated according to the instructions, and then added each sample to be tested in turn, mixed thoroughly and incubated in 37 °C oven

for 20-30 min, measured the OD value at wavelength 450 nm and calculated the SOD content.

Determination of mitochondrial MDA content in rat gastric tissues by TBA method

The mitochondria of fresh gastric tissue were taken, processed according to the instructions, and the supernatant was taken after centrifugation at 4000 rpm for 10 min. The absorbance value of each sample was measured at 532 nm and the MDA content was calculated.

Determination of mitochondrial ROS level in rat gastric tissue by chemofluorescence method

The mitochondria of fresh gastric tissue were taken, and the fluorescence intensity was measured at excitation wavelength 485 nm and emission wavelength 525 nm according to the procedure of the kit.

Determination of serum CS content in rat gastric tissue by ELISA

The rat serum CS content was determined according to the instructions of the kit. The absorbance A of each sample was read at 450 nm wavelength of the enzyme standard meter, and the standard curve was plotted to calculate the concentration value of each sample.

Observation of mitochondrial structure of ICC in rat gastric antrum tissue by transmission electron microscope (TEM)

Gastric antrum tissues were rapidly placed in 2.5% glutaraldehyde fixation for 2 h, rinsed and then fixed with 1% osmium fixative for 2 h, double distilled water rinsing, ethanol dehydration in steps for 10 min, block staining with 3% dioxin acetate in 70% ethanol at 4 °C, and after that, propylene oxide replacement, Epon812 embedding solution with propylene oxide infiltration (1:1, 2 h; 2:1, overnight), pure Epon812 embedding solution was infiltrated at 37 °C for 6 h. Sections were baked at 60 °C for 48 h, electronically stained with lead citrate, and observed and photographed by TEM (Hitachi, H-7650, Japan).

Observation of ckit, LC3 and VADC1, drp-1 and Tom20 expression in gastric antrum tissue by immunofluorescence

After xylene dewaxing, antigen repaired with 0.01 mol/L citrate buffer for 15 min, natural cooling to room temperature, 10% BSA blocked at room temperature for 1 h, primary antibodies (ckit, 1:200; LC3&VADC1, 1:200; Drp-1&Tom20, 1:200) were added overnight at 4 °C, added corresponding fluorescent secondary antibody (1:200) at room temperature and protected from light for 1 h. The nuclei were stained with DAPI for 5 min, and expressions was observed by fluorescence confocal microscopy (Leica TCS SP8 CARS, German).

Detection the expression of ckit and mitophagy-related proteins drp-1, p62, beclin-1, and LC3 in gastric antrum tissue by Western blot

10% SDS-PAGE was separated by electrophoresis for 90 min, the membrane was transferred by wet transfer method (300 mA, 30-90 min), 5% skimmed milk was closed for 2 h at room temperature in a shaker, rabbit anti-ckit, Drp-1, p62, Beclin-1, LC3 (1:1000) and β-actin (1:5000) were incubated overnight at 4 °C in a refrigerator in a shaker; the next day, the relevant secondary antibodies (1:2000) were incubated for 1 h at room temperature, the membrane was washed in TBST buffer, ultrasensitive enhanced chemiluminescence (ECL) luminescent solution was developed, the grayscale values of the protein bands were analyzed by Image J, and the target protein grayscale values/β-actin grayscale values were used to reflect the relative levels of the target proteins.

Statistical analysis

SPSS27.0 statistical software was used to analyze the data, and the results were expressed as mean ± standard deviation (means ± *SD*), and one-way analysis of variance (ANOVA) was used for comparison among multiple groups, with $p < 0.05$ representing a statistically significant difference.

Results

Effects of CHSGS on pathological changes of gastric antrum tissue in FD rats

Pathological changes of rat gastric sinus tissue were observed by HE staining to determine whether the modeling was successful. The gastric antrum tissue of rats in the control group had normal morphology, clear and complete hierarchical structure, distinct mucosal and muscular layers, and regular glandular structure; compared with the control group, a small amount of neutrophil infiltration was seen in the mucosal layer of the model group, with intact structural levels and no obvious pathological changes; there was no inflammatory cell infiltration in mdivi-1 group, mdivi-1 + CHSGS group and CHSGS group, and no pathological changes such as erosion and ulcer were found in each mucosal layer and muscular layer, as shown in Figure 1.

Effects of CHSGS on gastric emptying rate and small intestinal propulsion rate in FD rats

Semi-solid paste method for gastrointestinal motility. The gastric emptying rate (32.16 ± 4.85) and small intestinal propulsion rate (68.45 ± 6.89) in the model group was significantly decreased compared with the control group (52.84 ± 7.02; 82.44 ± 5.57) ($p < 0.01$). Compared with the model group, the gastric emptying rate and small intestinal propulsion rate in the mdivi-1 group (42.95 ± 5.32; 76.37 ± 7.31), mdivi-1 + CHSGS group (48.59 ± 9.48; 79.15 ± 8.16) and CHSGS group (45.07 ± 7.34; 76.59 ± 7.24) were significantly increased ($p < 0.05$, $p < 0.01$), as detailed in Table 1.

Effects of CHSGS on the expression of ckit in gastric antrum tissue of FD rats

Ckit is a tyrosine kinase receptor that specifically expresses ICC, and abnormalities in ICC number or function have important effects on gastrointestinal motility (Joung et al. 2021). The fluorescence results showed that the expression of ckit in the model

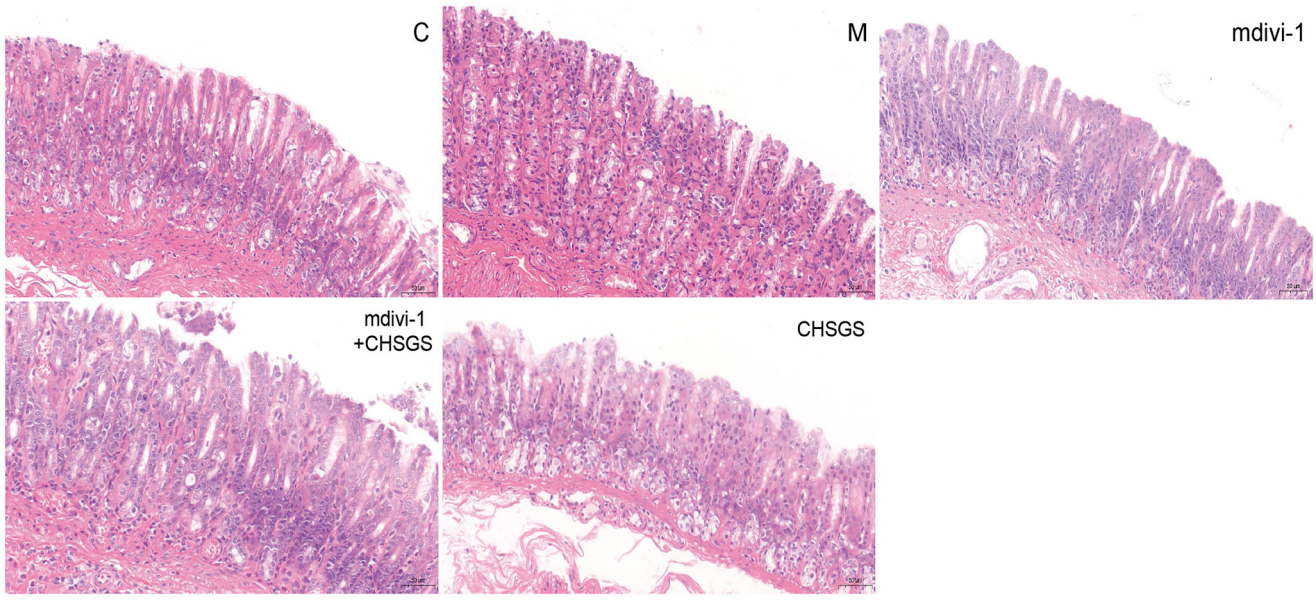

Figure 1. HE staining of rat gastric antrum tissue in each group (HE, ×200).

Table 1. Effects of CHSGS on gastric emptying rate and small intestinal propulsion rate in FD rats.

Group	*n*	Gastric emptying rate (%)	Small intestinal propulsion rat (%)
Control	8	52.84 ± 7.02	82.44 ± 5.57
Model	8	32.16 ± 4.85**	68.45 ± 6.89**
mdivi-1	8	42.95 ± 5.32##	76.37 ± 7.31#
mdivi-1 + CHSGS	8	48.59 ± 9.48##	79.15 ± 8.16##
CHSGS	8	45.07 ± 7.34##	76.59 ± 7.24#

Data were presented as means ± *SD*, compared with C, $^{**}p < 0.01$, compared with M, $^{\#}p < 0.05$, $^{\#\#}p < 0.01$.

group (6392.2 ± 950.8) was significantly decreased compared with the control group (43574.3 ± 5376.4) ($p<0.01$); compared with the model group, the expression of ckit in the mdivi-1 group (33532.8 ± 6627.5), mdivi-1 + CHSGS (38336.5 ± 3693.4) and CHSGS group (35065.2 ± 5246.5) was significantly increased ($p<0.01$), see Figure 2(A,B) for details. Western Blot results suggested that the expression of ckit in the model group (0.37 ± 0.06) was significantly decreased compared with the control group (0.76 ± 0.14) ($p<0.01$); compared with the model group, the expression of ckit in the mdivi-1, mdivi-1 + CHSGS and CHSGS groups was significantly increased (0.63 ± 0.13; 0.83 ± 0.12; 0.69 ± 0.09) ($p<0.01$), as detailed in Figure 2(C,D).

Effects of CHSGS on mitochondrial MDA、SOD content in gastric tissue of FD rats

MDA can indirectly reflect the degree of mitochondrial peroxidative damage (Tian et al. 2019). SOD can remove the harmful superoxide anion and achieve anti-oxidative stress (Yang et al. 2019; Liu et al. 2020). The mitochondrial MDA content in the model group was significantly increased (31.3 ± 1.9), whereas SOD content was significantly decreased (189.4 ± 12.8) compared with the control group (14.2 ± 2.0; 213.0 ± 11.4) ($p < 0.01$); compared with the model group, MDA content of mdivi-1 group (22.7 ± 1.5), mdivi-1 + CHSGS group (18.5 ± 1.4) and CHSGS group (25.2 ± 2.2) were significantly decreased ($p < 0.01$), and SOD content was significantly increased in the mdivi-1 group (204.5 ± 9.8), mdivi-1 + CHSGS group (217.1 ± 7.6) and CHSGS group (203.8 ± 14.6) ($p < 0.05$, $p < 0.01$), as detailed in Table 2.

Effects of CHSGS on serum CS, and mitochondrial ROS content in the gastric tissue of FD rats

Besides, CS and ROS have also the important role in maintaining normal mitochondrial function (Zhao et al. 2019; Ranjbarvaziri et al. 2021). The serum CS content in the model group (11.7 ± 2.5) was significantly decreased, and the mitochondrial ROS content was significantly increased (16467.7 ± 2509.4) compared with the control group (17.9 ± 3.1; 4385.1 ± 665.5) ($p < 0.01$); compared with the model group, serum CS content of mdivi-1 group (14.5 ± 2.0), mdivi-1 + CHSGS group (16.6 ± 3.2) and CHSGS group (15.7 ± 2.8) was significantly increased ($p < 0.05$, $p < 0.01$), and mitochondrial ROS content was significantly decreased in the mdivi-1 group (10497.8 ± 1902.0), mdivi-1 + CHSGS group (8183.5 ± 1374.6) and CHSGS group (9512.4 ± 918.8) ($p < 0.01$), as detailed in Table 3.

Effects of CHSGS on the ultrastructure of the ICC mitochondria in gastric antrum tissue of FD rats

Next, mitochondrial structure of ICC in rat gastric sinus tissues observed by TEM. In the control group, the morphological structure of ICC was clear, with long shuttle shape or oval shape, intact nuclear membrane, complete organelle structure, and a large number of mitochondria in the cytoplasm; in the model group, the shape of mitochondria was vague and branched, the mitochondria were swollen, dilated and vacuolated, and a large number of autophagic lysosomes were visible; the mitochondria were relatively intact, without obvious mitochondrial fission, and a small number of autophagic lysosomes could be seen in the mdivi-1 group; the mitochondrial morphology and structure of mdivi-1 + CHSGS group and CHSGS group was clearer, with higher cristae density, long shuttle-shaped mitochondria, intact nuclear membrane, and a small amount of mitochondrial fusion and division, see Figure 3 for details.

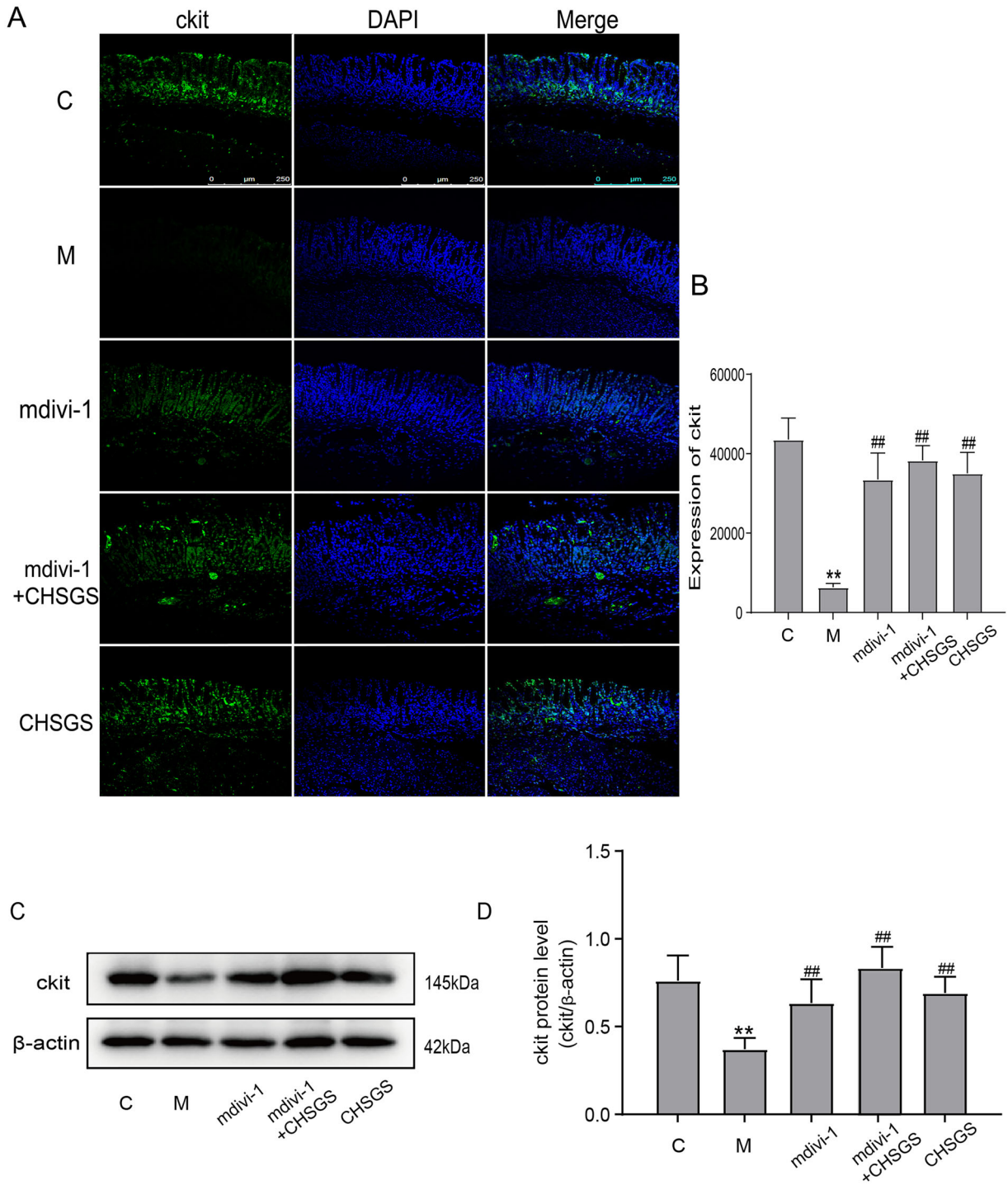

Figure 2. Expression of ckit in FD rats detected by Immunofluorescence and Western Blot. (A) Immunofluorescence. (B) Results of ckit Immunofluorescence. (C) Western Blot. (D) Results of ckit Western Blot. Data were presented as means ± *SD*, compared with C, $^{**}p < 0.01$, compared with M, $^{\#\#}p < 0.01$.

Table 2. Effects of CHSGS on mitochondrial MDA, SOD content in gastric tissue of FD rats.

Group	n	MDA (μmol/gprot)	SOD (U/mgprot)
Control	8	14.2 ± 2.0	213.0 ± 11.4
Model	8	31.3 ± 1.9**	189.4 ± 12.8**
mdivi-1	8	22.7 ± 1.5##	204.5 ± 9.8#
mdivi-1 + CHSGS 1 + CHSGS	8	18.5 ± 1.4##	217.1 ± 7.6##
CHSGS	8	25.2 ± 2.2##	203.8 ± 14.6#

Data were presented as means ± *SD*, compared with C, $^{**}p < 0.01$, compared with M, $^{\#}p < 0.05$, $^{\#\#}p < 0.01$.

Table 3. Effects of CHSGS on serum CS, and mitochondrial ROS content in the gastric tissue of FD rats.

Group	*n*	CS (U/L)	ROS (RFU/mgprot)
Control	8	17.9 ± 3.1	4385.1 ± 665.5
Model	8	11.7 ± 2.5**	16,467.7 ± 2509.4**
mdivi-1	8	14.5 ± 2.0#	10,497.8 ± 1902.0##
mdivi-1 + CHSGS 1 + CHSGS	8	16.6 ± 3.2##	8183.5 ± 1374.6##
CHSGS	8	15.7 ± 2.8##	9512.4 ± 918.8##

Data were presented as means ± *SD*, compared with C, $^{**}p < 0.01$, compared with M, $^{\#}p < 0.05$, $^{\#\#}p < 0.01$.

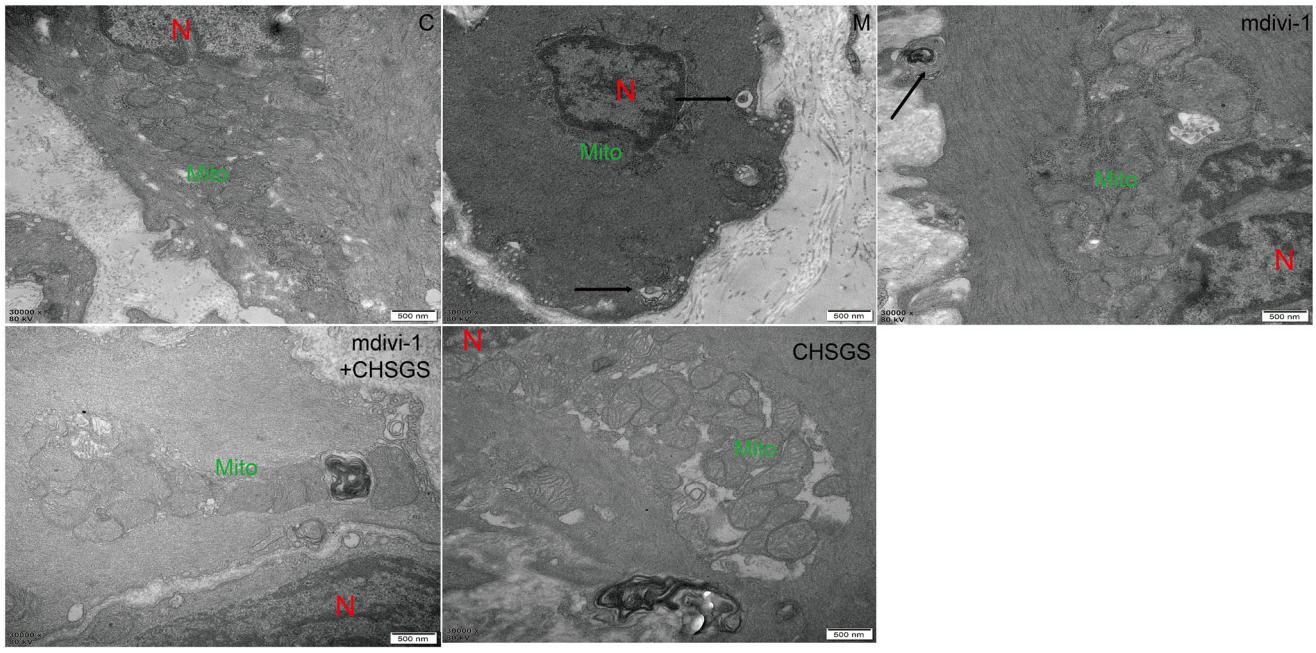

Figure 3. Effects of CHSGS on the ultrastructure of the ICC mitochondria in gastric antrum tissue of FD rats (TEM, ×30,000). N stands for nucleus, Mito for mitochondria, and autolysosomes were marked with arrows.

Effects of CHSGS on the fluorescence co-localization expression of LC3 and VDAC1, drp-1 and Tom20 in gastric antrum tissue of FD rats

To further confirm whether the mitochondria were wrapped by autophagosomes, we co-localized the expression of the mitochondrial outer membrane protein VDAC1 and the autophagosomal marker protein LC3; Drp-1, a key protein regulating mitophagy, with the mitochondrial marker Tom20 by Immunofluorescence, the co-localization expression of LC3 and VDAC1 was significantly increased in the model group (5955.4 ± 1599.0) compared with the control group (536.8 ± 147.8) ($p<0.01$); compared with the model group, whereas the co-localization expression was decreased in the mdivi-1, mdivi-1 + CHSGS and CHSGS groups (840.6 ± 169.9; 320.2 ± 115.8; 911.4 ± 322.2) ($p<0.01$), as detailed in Figure 4(A,B). The co-localization expression of Drp-1 and Tom20 was significantly increased in the model group (4946.4 ± 1471.5) compared with the control group (777.3 ± 136.8) ($p<0.01$); compared with the model group, the co-localization expression was significantly decreased in the mdivi-1, mdivi-1 + CHSGS and CHSGS groups (637.0 ± 224.3; 522.1 ± 187.5; 712.5 ± 220.3) ($p<0.01$), see Figure 4(C,D) for details.

Effects of CHSGS on the protein expression of mitochondrial drp-1, p62, beclin-1, and LC3 in FD rats

Finally, we speculated whether CHSGS could exert a pro-gastric motility effect by inhibiting Drp-1-mediated mitophagy. The protein expressions of mitochondrial Drp-1, Beclin-1, and LC3 in the model group (0.75 ± 0.20; 0.81 ± 0.09; 3.32 ± 1.12) were significantly increased compared with the control group (0.50 ± 0.17; 0.34 ± 0.10; 0.95 ± 0.49) ($p < 0.05$, $p < 0.01$), and the protein expression of p62 in the model group (0.44 ± 0.17) was significantly decreased compared with the control group (0.77 ± 0.12) ($p < 0.01$); compared with the model group, the protein expressions of Drp-1, Beclin-1, and LC3 in the mdivi-1 group (0.50 ± 0.25; 0.40 ± 0.13; 2.29 ± 0.86), mdivi-1 + CHSGS group (0.39 ± 0.10; 0.31 ± 0.12; 1.15 ± 0.46) and CHSGS group (0.54 ± 0.24; 0.66 ± 0.20; 2.00 ± 0.93) were decreased significantly ($p < 0.05$, $p < 0.01$) and the protein expression of p62 was significantly increased in the mdivi-1 group (0.73 ± 0.14), mdivi-1 + CHSGS group (0.79 ± 0.18) and CHSGS group (0.69 ± 0.11) ($p < 0.01$), as detailed in Figure 5.

Discussion

Functional dyspepsia (FD) is a non-organic disease with the main clinical symptoms of upper abdominal pain, epigastric distension, early satiety, belching, loss of appetite, nausea and vomiting, which can be persistent or recurrent. It's not clearly recorded in ancient Chinese medical books, but many records of "epigastric pain", "fullness" and "noisiness" are related to the clinical symptoms of FD. CHSGS is a classical representative formula for soothing the liver and regulating qi, and the etiology and clinical symptoms of the disease it treats coincide with the clinical symptoms of gastrointestinal dysfunctional diseases. In this formula, Bupleuri Radix is the ruling herb to regulate Qi in the liver, modern pharmacological study has shown that the main component of Bupleuri Radix, Chaihu Saponin A, has anti-inflammatory and anti-ulcer effects (Li et al. 2020). Cyperi Rhizoma and Chuanxiong Rhizoma invigorate blood circulation, remove blood stasis, move Qi and relieve pain as the ministerial medicines. Chuanxiong Rhizoma's main component, ferulic acid, is pro-gastric, antibacterial and anti-inflammatory, increases immune function, helps improve other concomitant gastrointestinal symptoms (Badary et al. 2006). Citri Reticulatae Pericarpium, Paeoniae Radix Alba, and Aurantii Fructus Immaturus regulate the Qi and stomach, soften the liver and relieve pain, eliminate gangrene and disperse nodules as adjuvants, modern pharmacology has confirmed that peony and its active ingredient paeoniflorin have gastrointestinal regulation and protection of gastric mucosa (Fang et al. 2012). Aurantii

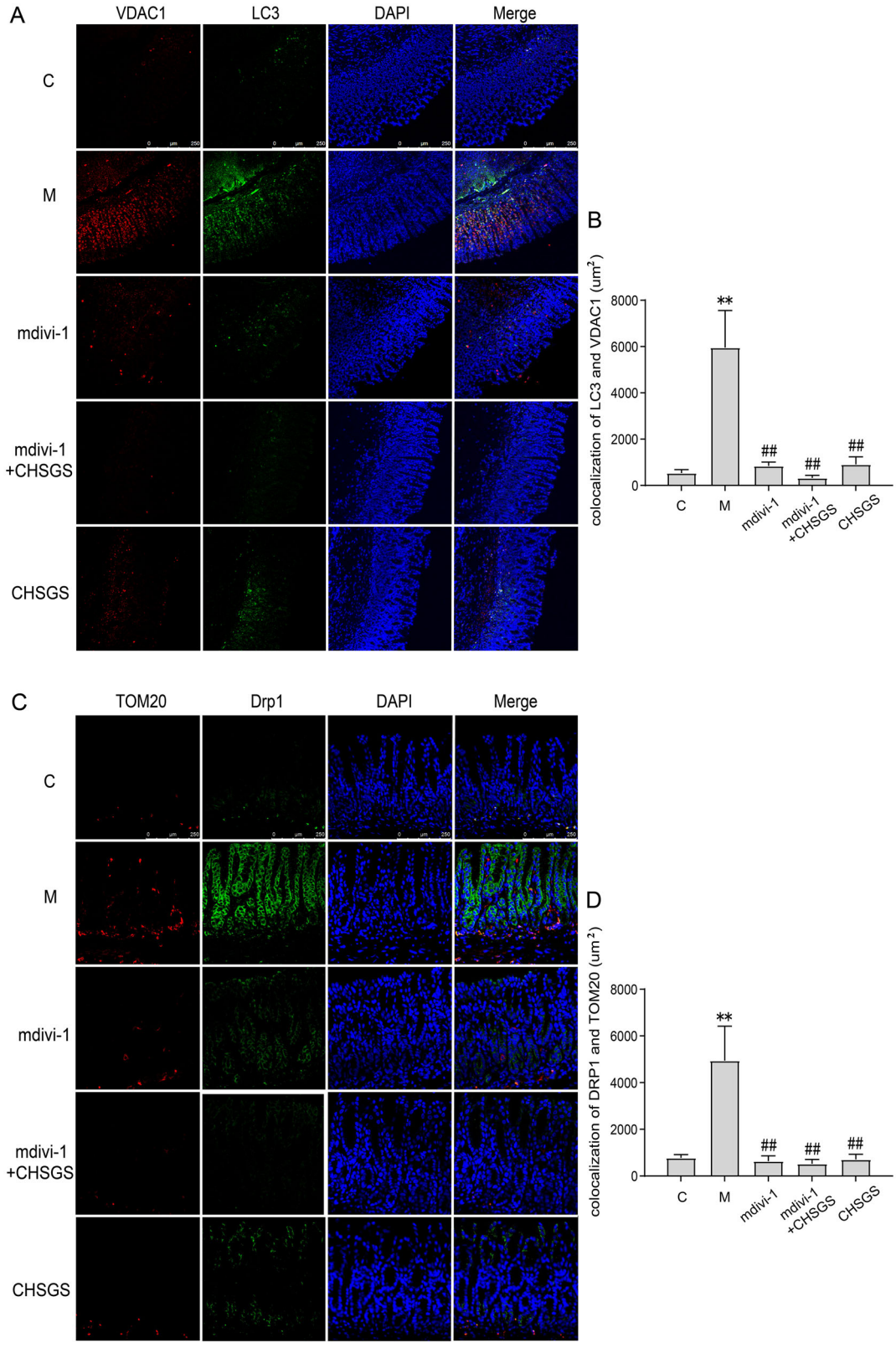

Figure 4. Effects of CHSGS on the fluorescence co-localization expression of LC3 and VDAC1, Drp-1 and Tom20 in gastric antrum tissue of FD rats. (A) Immunofluorescence of LC3 and VDAC1, (B) Colocalization of LC3 and VDAC1 Immunofluorescence. (C) Immunofluorescence of Drp-1 and Tom20. (D) Colocalization of Drp-1 and Tom20 Immunofluorescence. Data were presented as means ± *SD*, compared with C, $^{**}p < 0.01$, compared with M, $^{\#\#}p < 0.01$.

Fructus Immaturus, Citri Reticulatae Pericarpium, and its active ingredient hesperidin all have pro-gastrointestinal motility and antidepressant effects (Jia et al. 2022). Glycyrrhizae Radix et Rhizoma Praeparata cum Melle harmonizes the medicinal properties and acts as an enabler. Our group found that CHSGS promoted ICC activity by regulating smooth muscle cell (SMC) contraction; regulated stem cell factor (SCF)/ckit promoted ICC differentiation as well as phosphoInositide-3 kinase

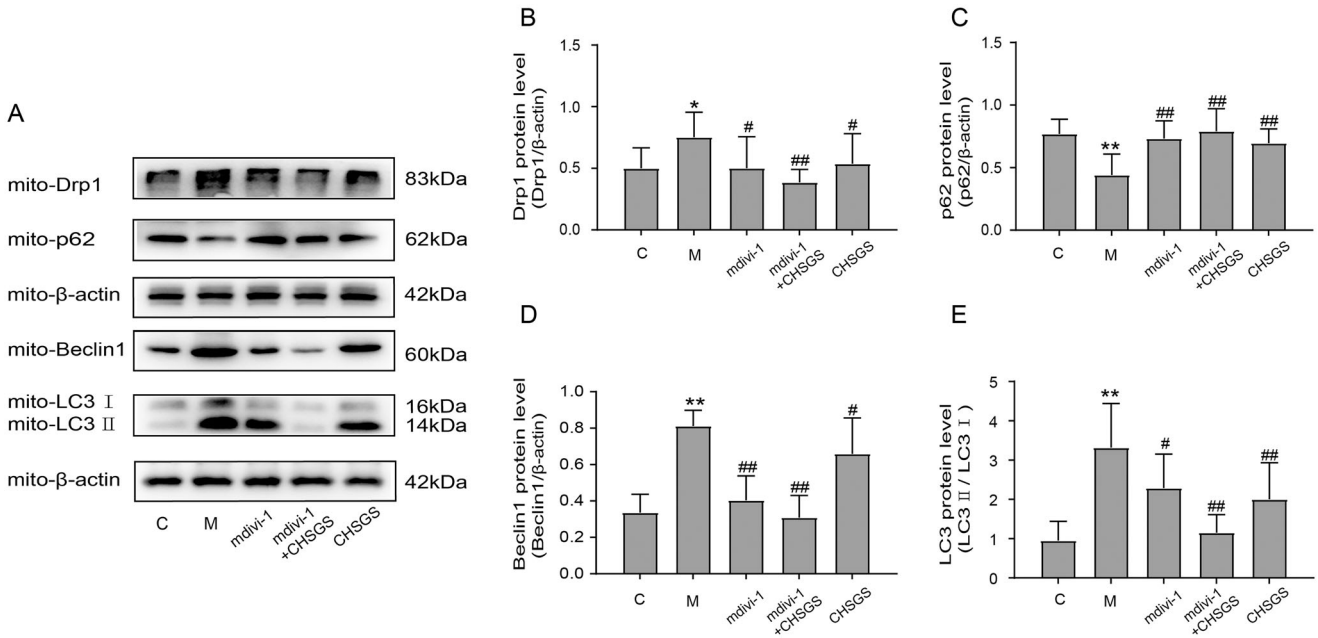

Figure 5. Effects of CHSGS on the protein expression of mitochondrial Drp-1, p62, Beclin-1, and LC3 in FD rats. (A) Western Blot. (B–E) Expression of Drp-1, p62, Beclin-1 and LC3. Data were presented as means ± *SD*, compared with C, $^{*}p < 0.05$, $^{**}p < 0.01$, compared with M, $^{\#}p < 0.05$, $^{\#\#}p < 0.01$.

(PI3K)/pyruvate dehydrogenase kinase 1 (PDK1) pathway to inhibit ICC autophagy, thus exerting a pro-gastrointestinal motility effect. Besides, we also found a large number of autophagic vesicles in the ICC of FD rats, accompanied by corresponding structural changes in mitochondria (Zhang et al. 2018; Tan et al. 2019). The results of this study showed that CHSGS could significantly increase the gastric emptying rate, small intestinal propulsion rate and ckit expression of FD rats, suggesting that CHSGS has the effect of promoting gastrointestinal motility and accelerating gastric emptying, which is consistent with our previous study.

Mitochondria are organelles with a double membrane structure and are the main source of cellular power (Annesley and Fisher 2019). It was found that more than 90% of ROS are produced in mitochondria during aerobic respiration and metabolism (Zorov et al. 2014). Mitochondria use the signaling pathway of ROS to regulate cellular hypoxia, proliferation and inflammatory responses (Zhao et al. 2019). When redox homeostasis is disrupted, in response, the key mitochondrial antioxidant enzyme, superoxide dismutase SOD, distributed in the mitochondrial matrix, will react with oxygen molecules to scavenge superoxide anions that are harmful to the organism to achieve antioxidant stress (Yang et al. 2019; Liu et al. 2020). MDA is a peroxidation product produced after ROS attack on unsaturated fatty acids, which has the role of reflecting the potential antioxidant capacity of mitochondria and can indirectly reflect the degree of mitochondrial peroxidative damage (Tian et al. 2019). CS is one of the key enzymes of the tricarboxylic acid cycle in the organism, and changes in its expression level directly affect mitochondrial ATP and free radical production, which has an important role in maintaining normal mitochondrial function (Ranjbarvaziri et al. 2021). There is evidence that a large number of mitochondrial structures are located in the cytoplasm of the rat myogastric tissue ICC by transmission electron microscopy, providing a large amount of energy for the pacing of gastrointestinal motility (Tan et al. 2019; Yu et al. 2021). Due to excessive stress, excessive autophagy occurs in mitochondria, which removes a large number of normal mitochondria, and the number of mitochondria decreases and their function is impaired, making them unable to provide energy for normal ICC activities, resulting in a decrease in the number of ICCs and thus causing gastric motility disorders. The results of this study suggested that CHSGS intervention reduced mitochondrial ROS and serum MDA levels, and increased serum SOD and CS content in gastric antrum tissue compared with the model group. The mitochondrial morphology and structure of ICC was clearer, and a small amount of mitochondrial fusion and division was found under TEM, suggesting that CHSGS intervention could reduce mitochondrial oxidative stress in FD rats.

Mitophagy is one of the forms of cellular autophagy, which refers to the process in which mitochondria in cells undergo depolarization and appear damaged under the action of external stimuli such as oxidative damage, and the damaged mitochondria are wrapped by autophagosomes and then fused with lysosomes, while completing the degradation of the damaged mitochondria (Springer and Macleod 2016; Chuang et al. 2020). Mdivi-1, a quinazolone derivative, is a newly discovered mitochondrial division protein inhibitor with the ability to inhibit Drp-1 self-assembly and mitochondrial division by inhibiting the activity of GTPase (Liu et al. 2020; Ding et al. 2022). Study found that mdivi-1 increases the survival of mitochondrial apoptosis in hepatocellular carcinoma (HCC) cells during hypoxia by blocking Drp-1-mediated mitophagy (Lin et al. 2020). Drp-1, a member of the kinesin superfamily, is recruited to the outer mitochondrial membrane under stress conditions and mediates membrane breakage through GTPase hydrolysis, triggering mitochondrial division and a decrease in mitochondrial MMP, leading to mitochondrial dysfunction (Gao et al. 2020). Studies have shown that under high glucose culture conditions, mitochondria of gastric cancer cells produce large amounts of ROS, SOD activity decreased, mitochondrial membrane potential decreased, Drp-1 protein expression increased, and mitophagy levels increased (Hao et al. 2019). As a key regulator in the mitochondrial fission process, Drp-1 exerts its fission-promoting function through four different steps (Qin et al. 2019; Wu et al. 2021). Mitochondrial fission is closely related to mitophagy, and various mitochondrial

fission regulatory proteins regulate mitophagy by interacting with LC3 adaptor proteins or LC3 receptors, which also regulate mitochondrial fusion by interacting with mitochondrial kinetic regulatory proteins (Chen et al. 2016; Yao et al. 2021). For example, Drp-1 interacts with LC3 receptors FUNDC1 and BCL2L13, which in turn undergo mitophagy (Wu et al. 2016). P62 is a specific substrate for mitophagy that directly binds LC3 and is selectively degraded by autophagy, negatively regulating mitochondrial autophagic activity (Sulkshane et al. 2021). Beclin-1, a key factor in evaluating mitochondrial autophagic activity, which can promote the conversion of LC3 I to LC3 II, accelerate the fusion of autophagosomes with lysosomes, and activate mitophagy (Jakhar et al. 2016). The results of this study suggested that CHSGS intervention downregulated the protein expression of mitochondrial Drp-1, Beclin-1, and LC3, and up-regulated the expression of mitochondrial p62. The above results showed that CHSGS could improve gastric motility in FD rats, maintain mitochondrial structural and functional homeostasis, regulate Drp-1-mediated ICC mitophagy, and thus effectively prevent and treat FD.

It is somewhat unfortunate that the specific mechanisms by which the Drp-1 signaling pathway and mitophagy in FD formation and progression have not been elucidated, and therefore Drp-1 silencing/overexpression experiments could be further performed.

Conclusions

CHSGS, as a classical formula for relieving the liver and regulating Qi, has been widely studied. In this study, we explored from the perspective of mitophagy and used mdivi-1, a mitophagy inhibitor, to intervene, and found that CHSGS could improve mitochondrial damage and promote gastric motility through Drp-1-mediated ICC mitophagy, which provided a new basis for FD research.

Author contributions

Jianghong Ling conceived and designed the study; Li Li and Qingling Jia completed the experiments and collected the data; Xiangxiang Wang, Yujiao Wang, Chenheng Wu, Jun Cong prepared the figures and revised the initial manuscript. All authors have read and approved the final manuscript.

Disclosure statement

No potential conflict of interest was reported by the author(s).

Funding

The work was supported by the National Natural Science Foundation of China [grant No. 82174309 and No. 81973774]; the National Administration of Traditional Chinese Medicine: 2019 Project of building evidence-based practice capacity for TCM [grant No. 2019XZZX-XH013].

References

Annesley SJ, Fisher PR. 2019. Mitochondria in health and disease. Cells. 8: 680.

Barberio B, Mahadeva S, Black CJ, Savarino EV, Ford AC. 2020. Systematic review with meta-analysis: global prevalence of uninvestigated dyspepsia according to the Rome criteria. Aliment Pharmacol Ther. 52(5):762–773.

Badary OA, Awad AS, Sherief MA, Hamada FM. 2006. *In vitro* and *in vivo* effects of ferulic acid on gastrointestinal motility: inhibition of cisplatin-induced delay in gastric emptying in rats. World J Gastroenterol. 12(33): 5363–5367.

Chen M, Chen ZH, Wang YY, Tan Z, Zhu CZ, Li YJ, Han Z, Chen LB, Gao RZ, Liu L, et al. 2016. Mitophagy receptor FUNDC1 regulates mitochondrial dynamics and mitophagy. Autophagy. 12(4):689–702.

Chuang KC, Chang CR, Chang SH, Huang SW, Chuang SM, Li ZY, Wang ST, Kao JK, Chen YJ, Shieh JJ. 2020. Imiquimod-induced ROS production disrupts the balance of mitochondrial dynamics and increases mitophagy in skin cancer cells. J Dermatol Sci. 98(3):152–162.

Ding J, Zhang ZH, Li S, Wang W, Du TY, Fang Q, Wang Y, Wang DW. 2022. Mdivi-1 alleviates cardiac fibrosis post myocardial infarction at infarcted border zone, possibly via inhibition of Drp-1-activated mitochondrial fission and oxidative stress. Arch Biochem Biophys. 718:109147.

Fang S, Zhu W, Zhang YM, Shu YQ, Liu P. 2012. Paeoniflorin modulates multidrug resistance of a human gastric cancer cell line via the inhibition of NF-κB activation. Mol Med Rep. 5(2):351–356.

Gao T, Zhang XH, Zhao J, Zhou F, Wang YY, Zhao Z, Xing JL, Chen BL, Li JB, Liu SJ. 2020. SIK2 promotes reprogramming of glucose metabolism through PI3K/AKT/HIF-1α pathway and Drp-1-mediated mitochondrial fission in ovarian cancer. Cancer Lett. 469:89–101.

Hao Y, Liu HM, Wei X, Gong X, Lu ZY, Huang ZH. 2019. Diallyl trisulfide attenuates hyperglycemia-induced endothelial apoptosis by inhibition of Drp-1-mediated mitochondrial fission. Acta Diabetol. 56(11):1177–1189.

Ford AC, Mahadeva S, Carbone MF, Lacy BE, Talley NJ. 2020. Functional dyspepsia. Lancet. 396(10263):1689–1702.

Jakhar R, Paul S, Bhardwaj M, Kang SC. 2016. Astemizole-histamine induces beclin-1-independent autophagy by targeting p53-dependent crosstalk between autophagy and apoptosis. Cancer Lett. 372(1):89–100.

Jia QL, Li L, Wang XX, Wang YJ, Jiang KL, Yang KM, Cong J, Cai G, Ling JL. 2022. Hesperidin promotes gastric motility in rats with functional dyspepsia by regulating Drp1-mediated ICC mitophagy. Front Pharmacol. 13: 945624.

Joung JY, Choi SH, Son CG. 2021. Interstitial cells of cajal: potential targets for functional dyspepsia treatment using medicinal natural products. Evid Based Complement Alternat Med. 2021:9952691.

Hou LW, Fang JL, Zhang JL, Wang L, Wu D, Wang JY, Wu MZ, Rong PJ. 2022. Auricular vagus nerve stimulation ameliorates functional dyspepsia with depressive-like behavior and inhibits the Hypothalamu-Pituitary-Adrenal axis in a rat model. Dig Dis Sci. 67(10):4719–4731.

Li J, Han JF, Lv J, Wang SJ, Qu L, Jiang YF. 2020. Saikosaponin A-induced gut microbiota changes attenuate severe acute pancreatitis through the activation of Keap1/Nrf2-ARE antioxidant signaling. Oxid Med Cell Longev. 2020:9217219.

Liang QK, Yan Y, Mao LF, Du XJ, Liang JJ, Liu JH, Wang LD, Li HF. 2018. Evaluation of a modified rat model for functional dyspepsia. Saudi J Gastroenterol. 24(4):228–235.

Lin XH, Qiu BQ, Ma M, Zhang R, Hsu SJ, Liu HH, Chen J, Gao DM, Cui JF, Ren ZG, et al. 2020. Suppressing DRP-1-mediated mitochondrial fission and mitophagy increases mitochondrial apoptosis of hepatocellular carcinoma cells in the setting of hypoxia. Oncogenesis. 9(7):67.

Liu RJ, Wang SC, Li M, Ma XH, Jia XN, Bu Y, Sun L, Yu KJ. 2020. An inhibitor of DRP-1 (Mdivi-1) alleviates LPS-induced septic AKI by inhibiting NLRP3 inflammasome activation. Biomed Res Int. 2020:2398420.

Liu Z, Wang XF, Li L, Wei GG, Zhao M. 2020. Hydrogen sulfide protects against paraquat-induced acute liver injury in rats by regulating oxidative stress, mitochondrial function, and inflammation. Oxid Med Cell Longev. 2020:6325378.

Madisch A, Andresen V, Enck P, Labenz J, Frieling T, Schemann M. 2018. The diagnosis and treatment of functional dyspepsia. Dtsch Arztebl Int. 115(13):222–232.

Mizushima N, Komatsu M. 2011. Autophagy: renovation of cells and tissues. Cell. 147(4):728–741.

Qin X, Zhao Y, Gong J, Huang WY, Su H, Yuan F, Wang DK, Li JB, Zou X, Xu LJ, et al. 2019. Berberine protects glomerular podocytes via inhibiting Drp-1-mediated mitochondrial fission and dysfunction. Theranostics. 9(6): 1698–1713.

Ranjbarvaziri S, Kooiker KB, Ellenberger M, Fajardo G, Zhao M, Vander Roest AS, Woldeyes RA, Koyano TT, Fong R, Ma N, et al. 2021. Altered cardiac energetics and mitochondrial dysfunction in hypertrophic cardiomyopathy. Circulation. 144(21):1714–1731.

Rovira-Llopis S, Bañuls C, Diaz-Morales N, Hernandez-Mijares A, Rocha M, Victor VM. 2017. Mitochondrial dynamics in type 2 diabetes: pathophysiological implications. Redox Biol. 11:637–645.

Springer MZ, Macleod KF. 2016. In brief: mitophagy: mechanisms and role in human disease. J Pathol. 240(3):253–255.

Sulkshane P, Ram J, Thakur A, Reis N, Kleifeld O, Glickman MH. 2021. Ubiquitination and receptor-mediated mitophagy converge to eliminate oxidation-damaged mitochondria during hypoxia. Redox Biol. 45:102047.

Tan RQ, Zhang Z, Ju J, Ling JH. 2019. Effect of Chaihu shugan powder-contained serum on glutamate-induced autophagy of interstitial cells of cajal in the rat gastric antrum. Evid Based Complement Alternat Med. 2019:7318616.

Tian L, Cao WJ, Yue RJ, Yuan Y, Guo XH, Qin DM, Xing JH, Wang XC. 2019. Pretreatment with Tilianin improves mitochondrial energy metabolism and oxidative stress in rats with myocardial ischemia/reperfusion injury via AMPK/SIRT1/PGC-1 alpha signaling pathway. J Pharmacol Sci. 139(4):352–360.

Wauters L, Talley NJ, Walker MM, Tack J, Vanuytsel T. 2020. Novel concepts in the pathophysiology and treatment of functional dyspepsia. Gut. 69(3):591–600.

Wu W, Jing DD, Huang X, Yang WB, Shao ZW. 2021. Drp-1-mediated mitochondrial fission is involved in oxidized low-density lipoprotein-induced AF cella poptosis. J Orthop Res. 39(7):1496–1504.

Wu WX, Lin CX, Wu K, Jiang L, Wang XJ, Li W, Zhuang HX, Zhang XL, Chen H, Li SP, et al. 2016. FUNDC1 regulates mitochondrial dynamics at the ER-mitochondrial contact site under hypoxic conditions. Embo J. 35(13):1368–1384.

Wu ZY, Lu XF, Zhang SS, Zhu CY. 2020. Sini-San regulates the NO-cGMP-PKG pathway in the spinal dorsal horn in a modified rat model of functional dyspepsia. Evid Based Complement Alternat Med. 2020:3575231.

Yang F, Pei RN, Zhang ZW, Liao JZ, Yu WL, Qiao N, Han QY, Li Y, Hu LMY, Guo J, et al. 2019. Copper induces oxidative stress and apoptosis through mitochondria-mediated pathway in chicken hepatocytes. Toxicol in Vitro. 54:310–316.

Yao RQ, Ren C, Xia ZF, Yao YM. 2021. Organelle-specific autophagy in inflammatory diseases: a potential therapeutic target underlying the quality control of multiple organelles. Autophagy. 17:385–401.

Yi ZR, Jia QL, Lin YL, Wang YJ, Cong J, Gu ZJ, Ling JH, Cai G. 2022. Mechanism of Elian granules in the treatment of precancerous lesions of gastric cancer in rats through the MAPK signalling pathway based on network pharmacology. Pharm Biol. 60(1):87–95.

Yu H, Liu YQ, Chu M, Si Y, Ye YQ, Ge TT, Zhao HQ, Zhang H. 2021. Structural relationships between interstitial cells of cajal and smooth muscle cells/nerve fibers in the gastric muscularis mucosae of Chinese giant salamander. Microsc Microanal. 27(1):227–235.

Zhang LM, Zeng LJ, Deng J, Zhang YQ, Wang YJ, Xie TY, Ling JH. 2018. Investigation of autophagy and differentiation of myenteric interstitial cells of Cajal in the pathogenesis of gastric motility disorders in rats with functional dyspepsia. Biotechnol Appl Biochem. 65(4):533–539.

Zhao RZ, Jiang S, Zhang L, Yu ZB. 2019. Mitochondrial electron transport chain, ros generation and uncoupling (Review). Int J Mol Med. 44(1):3–15.

Zorov DB, Juhaszova M, Sollott SJ. 2014. Mitochondrial reactive oxygen species (ROS) and ros-induced ros release. Physiol Rev. 94(3):909–950.

Zhu J, Tong H, Ye X, Zhang J, Huang Y, Yang M, Zhong L, Gong Q. 2020. The effects of low-dose and high-dose decoctions of fructus aurantii in a rat model of functional dyspepsia. Med Sci Monit. 26:e919815.